DEVELOPMENT OF A 3D COMPUTER MODEL FOR DEFIBRILLATION STUDIES BASED ON HISTOLOGICAL RABBIT DATA

A.J. Prassl* and G. Plank*

* Medical University of Graz/Institute of Biophysics, Graz, Austria

anton.prassl@meduni-graz.at

Abstract: Cardiac fibrillation is the complete disorganization of the heart's electrical activity. The administration of an electrical shock (defibrillation) is the only known effective therapy to restore the heart's normal rhythm. Although defibrillation is successfully applied in clinical practice, the underlying mechanisms remain poorly understood. Computer simulations of defibrillation shocks are among the most elegant methods to unravel this phenomenon, however, todays models are still too simplistic in several regards. Although whole ventricle computer simulations have become tractable, essential anatomical and functional features are still missing in these models. To increase the predictive power of computer simulations missing features have to be added. In this study, we developed a first version of a computer model of rabbit ventricles which is suited for defibrillation studies. At the current state, gross anatomy and fiber orientations are accurately model based on MRI data. In subsequent steps, the model will be complemented by incorporating micro-anatomical details like vessels and cleavage planes.

Keywords: **3D modeling, Non-Uniform Rational B-Splines, mesh generation, bidomain, defibrillation.**

Introduction

The administration of strong electrical shocks, referred to as electrical defibrillation, is the only known therapy to restore a sinus rhythm in a fibrillating heart. Although defibrillation is successfully applied in clinical practice since world war II, key aspects of the underlying biophysical mechanism remain poorly understood. Computer models have demonstrated to be a very valuable tool to gain insights into these mechanisms, however, defibrillation studies with such models are demanding for two reasons: First, bidomain formulations which account for current flow in both the intracellular and interstitial/extracellular domain are better suited for such studies than the computationally significantly less expensive and theoretically less general monodomain formulations. Besides, the computation of a shock enforces very small time steps down to $1\mu s$ and less which further increases the computational burden. Further, there are additional requirements regarding the mesh quality. The use of unstructured grids is almost mandatory to allow a smooth representation of the organ boundaries, since boundaries defined on structured grids tend to cause artifactual currents due to tip effects at the jagged surface. However, although mesh generation using unstructured grids is not as straightforwardly accomplished as with structured grids, there are major advantages too. Fine discretization is required within the myocardial volume only, whereas outside the tissue, in the bath or within the blood filled cavities, much coarser discretizations are acceptable. With increasing distance from a myocardial surface the spatial resolution of a mesh can be reduced without decreasing the accuracy of the solution while the number of unknowns can be reduced significantly.
The goal of this study is to develop a method which transforms a mesh, defined on a structured grid, into an unstructured mesh pursuing two major goals, first, to allow smooth representation of the organ boundaries, and, secondly, to achieve a significant reduction of the number of unknowns and thus reduce the computation workload associated with the elliptic portion of the bidomain equations.

Materials and Methods

The development of the computer model is based on available MRI data of rabbit's ventricular geometry [1]. MRI data are voxel-based and thus can easily be transformed into a hexahedral mesh. However, due to the edgy representation of surfaces, hexahedral meshes are unsuited for defibrillation studies since artifactual currents arising at the element edges are inevitable. Consequently, to obtain a smooth representation of the organs boundary the hexahedral mesh was transformed to a tetrahedral mesh as follows:

Edge Detection: Points on the myocardial surfaces were obtained by differentiating binary images of the cross-sections. Sorting the point set in each cross-section led to an oriented boundary curve. Dot pitches greater than the spatial discretization served as criterion to separate myocardial surfaces. The location of the boundary's barycenters in each cross-section allowed the discrimination of left and right endocardium as well as of the epicardium (see Fig. 1).

Surface Constitution and Smoothing: A parametric approach with Non-Uniform Rational B-Splines [2] was chosen to represent the global surfaces. On each boundary curve, N equidistantly distributed points were se-

ISSN: 1727-1983

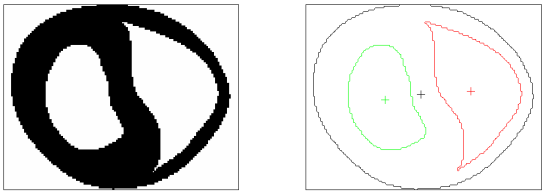

Figure 1: *Left:* Binary image generated from one hexahedral mesh layer. *Right:* Boundary curves were obtained from differentiated binary images. The barycenters served as criterion to discriminate epicardial (black), left (green) and right (red) endocardial boundaries.

lected. N points in M sections formed the set $\mathbf{S}$ of $M \times N$ control points. The net of $\mathbf{S}$ control points was parameterized using NURBS. $\mathbf{S}$ vertices and two knot vectors (discretization of the parameter space along u and v) defined the surfaces of the endocardial cavities and the epicardium in 3D space (see Fig. 2).

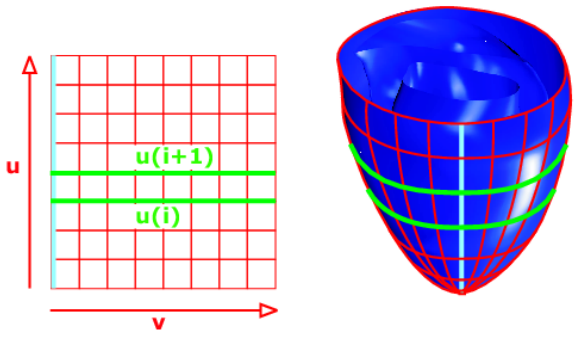

Figure 2: *Left:* Two-dimensional (u,v) NURBS parameter space. *Right:* Equivalent transformation of (u,v) parameters into the real world coordinate system.

Smooth organ surfaces were mandatory for the defibrillation simulations to avoid artifactual currents arising at the element edges. Varying the NURBS order allowed to control the smoothness of the surfaces as can be seen in Fig. 3.

Surface Triangulation: The NURBS parameter space was discretizised along u (direction apex to base) and v (circumferential direction) to result in the desired discretization Δs ($\approx 250\mu m$) in real world coordinates. The summation of all Δs defined the boundary curve length L. The number of grid points $\tilde{N}(u_i)$ on each smoothed boundary curve was computed from the quotient of curve length L and the desired spatial discretization Δs, where $\tilde{N}(u_i) \approx L/\Delta s$. The number of nodes along the circumference changed from layer to layer. Before triangulating the surface, nodes were shifted in circumferential direction to avoid any "funny" surface elements. Quadrilaterals placed between neighboring boundary curves u_i and u_{i+1} were used to form the surface elements. $\Delta\tilde{N}$ triangles were inserted to account for unequal curve lengths,

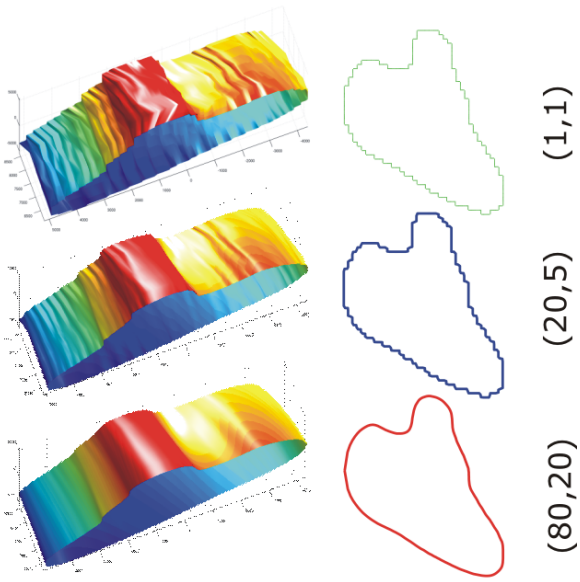

Figure 3: Influence of different NURBS order settings on the smoothness of the surfaces.

where

$$\Delta\tilde{N} = \tilde{N}(u_{i+1}) - N(u_i) \qquad (1)$$

FEM-Mesh Generation: Commercial software *Hypermesh* (Altair Engineering, Germany) was used to generate a volume tetrahedral mesh with the triangulated epicardial and endocardial surfaces as boundaries. Three different domains were created: the endocardial cavities (*I*), the myocardium (*II*) and the bath (*III*) (see Fig. 4). The dimensions for the bath volume were chosen by adding $2mm$ on each side of the rabbit's heart. Memory requirements enforced the decomposition of the surfaces into subdomains of $1mm$ height. These were meshed sequentially and put together again. Due to numerical considerations and in order to keep solution times low, the tetrahedral mesh coarsens from the myocardial surfaces towards the areas *I* and *III*. No adaptivity of the finite elements was allowed inside the myocardium.

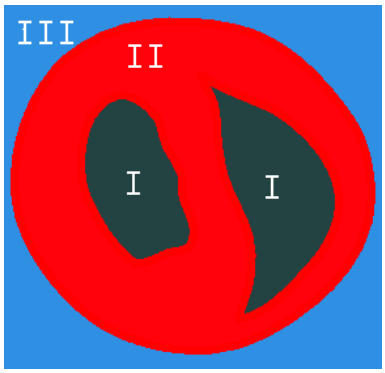

Figure 4: Domain decomposition. No adaptivity during element generation was allowed in area II.

ISSN: 1727-1983

Fiber Interpolation: The fiber orientations were mapped from the hexahedral grid onto the tetrahedral grid. The mapping was carried out componentwise via nearest neighbor interpolation using the Matlab routine *griddata3* (The MathWorks Inc., Natick, USA):

$$dx(\vec{r}_0) \rightarrow dx(\vec{r}_n) \quad (2)$$
$$dy(\vec{r}_0) \rightarrow dy(\vec{r}_n) \quad (3)$$
$$dz(\vec{r}_0) \rightarrow dz(\vec{r}_n), \quad (4)$$

where $\vec{r}_0$ is the fiber orientation on the original hexahedral grid and $\vec{r}_n$ the corresponding orientations onto the unstructured grid.

Numerical Solution: Induction of reentry and the subsequent application of a defibrillation shock was simulated using the software *CARP* [3]. The numerical method was described in detail in [4]. The dynamic membrane behavior during normal excitation spread and during shock delivery was based on [5] and [6].

Results

Surface Constitution and Smoothing: MRI data of rabbit's ventricular geometry was transformed into a hexahedral mesh. The extracted boundary curves were parameterized and smoothed using NURBS (see Fig. 5).

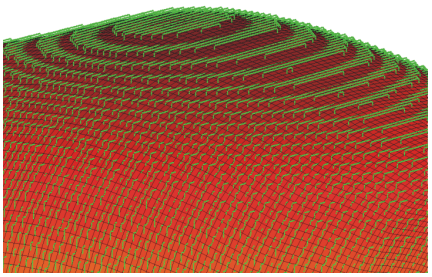

Figure 5: View on smooth epicardial surface of the rabbit heart. Hexahedral surface vertices (structured grid) are plotted in green dots.

FEM-Mesh Generation: Commercial software generated a volume tetrahedral mesh onto an unstructured grid. A summary of the finite element quantities and number of vertices is shown in Tab. 1.

Table 1: Comparison of finite element numbers and vertices distribution in raw data and developed 3D model

	Myocardium	**Total**
Hexahedra	470.201	1.732.599
Vertices	522.841	1.776.320
Tetrahedra	3.073.529	5.082.272
Vertices	547.680	862.515

The generation of quality volumetric meshes closely corresponds with geometric characteristics, such as the edge length distribution (see Tab. 2).

Table 2: Analysis of intra- and extramyocardial tetrahedral elements in reference to its edge length distribution

Parameter	**Myocardium**	**Cavities, Bath**
Mean value μ	$275.81\mu m$	$390.18\mu m$
Std. Deviation σ	$49.01\mu m$	$175.40\mu m$

Coarser tetrahedral elements were produced in the endocardial cavities and the bath as it is shown in Fig. 6.

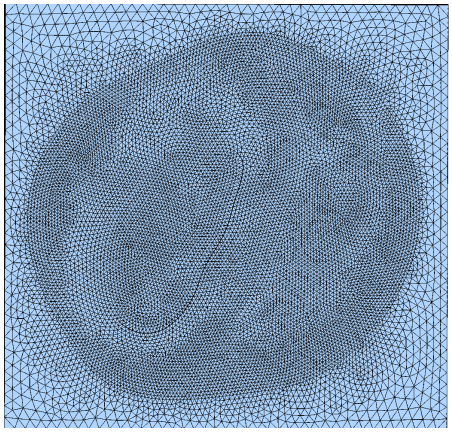

Figure 6: The view to the heart's basis shows the size variation of the finite elements: high density of similarly sized surface elements in myocardial areas - coarsening of the elements in the surrounding area.

Fiber Interpolation: The fiber orientations were interpolated from the hexahedral grid onto the unstructured tetrahedral grid with the Matlab function *griddata3* (see Fig. 7).

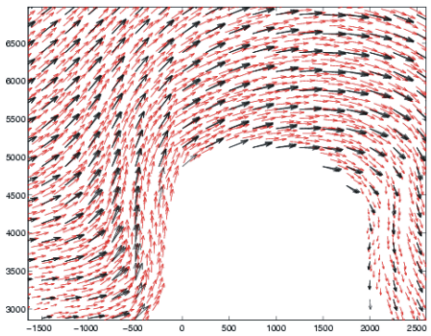

Figure 7: Mapping of fiber orientations between hexahedral grid (black arrows) and tetrahedral grid (red arrows).

Shock Delivery: Consistent with published data, despite the use of plate electrodes which produce a homogeneous external electric field, virtual electrodes (see Fig. 8) were observed next to cathodal and anodal polarization under the electrodes as a consequence of unequal

ISSN: 1727-1983

anisotropy ratios between intracellular and interstitial domain. The rise of transmembrane voltages were limited by electroporation and a hypothetical I_a current which was incorporated to account for the membrane's asymmetric response to shocks. Artifactual effects like observed when using voxel-based hexahedral meshes were not observed.

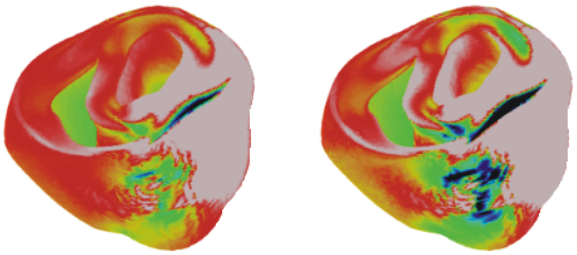

Figure 8: Next to cathodal and anodal polarizations, virtual electrode polarizations of opposite polarity due to the presence of unequal anisotropy ratios, were observed.

Discussion

Many mesh generation problems involve the formation of elements on arbitrary three-dimensional surfaces [7]. 3D surfaces are typically represented by NURBS. The development of our 3D computer model is based upon this approach. The modification of the NURBS order provides an elegant method to smooth the organ surfaces (see Fig. 5), where the endocardial cavities and the epicardium form not intersecting, closed boundary curves. However, basal cross-sections of the MRI data which do not fulfill this constraint, were not meshed.
The mesh quality can have a considerable impact on the computational analysis in terms of the quality of the solution and the time needed to obtain it. Different parameters, e.g. the skew, the shape, the volume or the edge length distribution estimate the mesh quality. The commercial mesh generator created tetrahedral elements in the myocardium with mean edge length $\mu = 275.81\mu m$ and standard deviation $\sigma = 49.01\mu m$ (see Tab. 2). This suffices the desired mean edge length of $250\mu m$.
The second major goal of this study, besides the smoothing of the organ boundaries, was to reduce the number of unknowns in order to relieve the computation workload. The total amount of vertices was bisected (see Tab. 1), whereas the vertices within the myocardium nearly remained the same.

Conclusions

The development of a 3D computer model based on MRI data of a rabbit heart was presented. As the edgy representation of the underlying hexahedral volume mesh is unsuited for defibrillation simulations, a transformation onto an unstructured grid was found working off following steps: boundary detection, surface creation using NURBS, surface triangulation, finite element generation in *Hypermesh* and interpolation of the fiber orientations between structured and unstructured grid under Matlab. The choice of the NURBS order allowed to control the smoothness of the epi- and endocardial surfaces.
In a further step, the model will be validated with experimental data to get good agreement regarding conduction velocity and action potential duration. To locally adjust these parameters the model has to account for cardiac heterogeneities in both function and structure. More details of the cardiac ultrastructure (connective tissue, vessels) and the functional heterogeneity (transmural and apicobasal) will be included in later versions of the model. Defibrillation studies force to solve the bidomain equations in nano-second time steps. The numerical solution of these equations with millions of unknown variables and up to 50.000 time steps for one single shock challenges even state-of-the-art technology.

Acknowledgment

This work was supported by Austrian National Research Foundation FWF under grant R21-N04.

References

[1] F. J. VETTER and A. D. MCCULLOCH. Three-dimensional analysis of regional cardiac function: a model of rabbit ventricular anatomy. *Prog Biophys Mol Biol*, 69(2-3):157–183, 1998.
[2] PIEGL, L. and TILLER, W. *The NURBS Book, second edition*. Springer Verlag, Berlin, Heidelberg, New York, 1997.
[3] EDWARD J VIGMOND, MATT HUGHES, G. PLANK, and L. JOSHUA LEON. Computational tools for modeling electrical activity in cardiac tissue. *J Electrocardiol*, 36 Suppl:69–74, 2003.
[4] MATTHEW G HILLEBRENNER, JAMES C EASON, and NATALIA A TRAYANOVA. Mechanistic inquiry into decrease in probability of defibrillation success with increase in complexity of preshock reentrant activity. *Am J Physiol Heart Circ Physiol*, 286(3):H909–H917, Mar 2004.
[5] J. L. PUGLISI and D. M. BERS. LabHEART: an interactive computer model of rabbit ventricular myocyte ion channels and Ca transport. *Am J Physiol Cell Physiol*, 281(6):C2049–C2060, Dec 2001.
[6] K. A. DEBRUIN and W. KRASSOWSKA. Electroporation and shock-induced transmembrane potential in a cardiac fiber during defibrillation strength shocks. *Ann Biomed Eng*, 26(4):584–596, 1998.
[7] P. W. DE BRUIN, V. J. DERCKSEN, F. H. POST, A. M. VOSSEPOEL, G. J. STREEKSTRA, and F. M. VOS. Interactive 3D segmentation using connected orthogonal contours. *Comput Biol Med*, 35(4):329–346, May 2005.

ISSN: 1727-1983